Journal of the European Ceramic Society 45 (2025) 117244

Contents lists available at ScienceDirect

Journal of the European Ceramic Society

journal homepage: www.elsevier.com/locate/jeurceramsoc

Iron-manganese crystalline phases developed in high lead glazes during firing

J. Molera [a,*], M. Colomer [b], O. Vallcorba [c], T. Pradell [d]

[a] MECAMAT Research Group, Facultat de Ciències, Tecnologia i Enginyeries. Universitat de Vic – Universitat Central de Catalunya, C. de la Laura, 13, Vic 08500, Spain
[b] Universitat de Barcelona, Dept. Educació Lingüística, Científica i Matemàtica. Campus Mundet, Passeig de la Vall d'Hebron 171, Barcelona 08035, Spain
[c] ALBA Synchrotron Light Source, Carrer de la Llum 2-26,Cerdanyola del Vallès, Barcelona 08290, Spain
[d] Universitat Politècnica de Catalunya - BarcelonaTech, Departament de Física, BRCMSE, Campus Diagonal-Besòs, Av. Eduard Maristany 10-14, Barcelona 08019, Spain

ARTICLE INFO

Keywords:
High-temperature synchrotron powder X-Ray diffraction
Lead glaze
PbO-SiO_2-Fe_2O_3-MnO-Al_2O_3-MgO-CaO
Barysilite
Ganomalite
Andradite
Melanotekite
Kentrolite
Magnetoplumbite
Jacobsite
Haematite
Braunite
Pyroxene
Microstructure

ABSTRACT

Lead glazes have been coloured and decorated with iron and manganese oxides since ancient times. During firing, these pigments react and form new crystalline compounds such as haematite, andradite, melanotekite, kentrolite, braunite, jacobsite and magnetoplumbite which have been identified in lead-glazed ceramics from the 11th to 17th centuries. To determine the sequence of formation of these pigments, an X-ray powder diffraction experiment was conducted at the ALBA synchrotron up to 928°C with various mixtures. The influence of Al_2O_3, CaO, and MgO was also studied. The sequence of crystalline phase formation in different systems was established, and laboratory recreations of glazed ceramics at temperatures from 850°C to 1020°C were analysed using optical and electronic microscopy. Understanding the sequence of formation of iron and manganese crystals in lead glazes helps to elucidate ancient production techniques and the final appearance of the glazes.

1. Introduction

Ceramic glazes have been decorated and coloured with iron pigments for centuries, with iron oxides playing a particularly important role as a colouring agent since Roman times, and certainly during the Middle Ages. Iron oxide, in small quantities (0.5 to 4 % Fe_2O_3) is responsible for the yellow hues in lead glazes, while higher concentrations (4–10 % Fe_2O_3) produce brown colours, and with even higher concentrations almost black, mat appearance (non-glossy appearance). In the latter case, iron compounds crystallise in the glazes. In combination with manganese oxide, the colour becomes black and other crystalline phases are formed. The composition of raw materials, including the glaze, ceramic body, and pigment, along with specific firing conditions, influences the nature, size, and distribution of the resulting crystalline phases and the final colour.

The identification of neoformed crystals in ancient glazes is a well-established method for studying historical ceramic production [1]. These crystalline phases not only determine the aesthetic qualities of the glaze, such as colour and texture but also provide valuable insights into ancient ceramic production techniques. This information can be used to identify production centres but also to distinguish between authentic pieces from imitations, since the adoption of a new glazed ware that mimics the appearance of an imported style does not necessarily imply the use of identical production methods or materials. Variations in raw materials, glazing techniques, and firing conditions can result in distinct crystalline compositions and microstructures that differ from the originals.

Various iron-rich crystallites have been reported in ceramic glazes dating from the 11th to the 17th centuries. Both haematite and melanotekite ($Pb_2Fe^{3+}_2O_2(Si_2O_7)$) have been identified in 19th-century French imitations of the Ligurian Taches Noires ware from Joques (Provence, France) [2], as well as in the imperial red overglaze

* Correspondence to: Universitat de Vic-Universitat Central de Catalunya
E-mail address: judit.molera@uvic.cat (J. Molera).

https://doi.org/10.1016/j.jeurceramsoc.2025.117244
Received 7 November 2024; Received in revised form 26 January 2025; Accepted 28 January 2025
Available online 29 January 2025

decoration from 15th-century China [3]. DiFebo's research [2] suggests that in SiO_2-PbO-Fe_2O_3 glazes, melanotekite begins to melt below 930°C. As it melts, any excess iron promotes the formation of additional haematite crystals, typically in the form of hexagonal platelets.

Roisine et al. (2017) [4] replicated the Bernard Palissy glaze and found that, regardless of the cooling rate, at around 875°C, primary haematite from the raw material gradually reacts with the lead silicate melt to form melanotekite ($Pb_2Fe_2^{3+}O_2(Si_2O_7)$). Between 875°C and 1023°C, melanotekite dissolves in the melt, while secondary haematite recrystallises. At 1023°C, the system exceeds the liquidus temperature, and all haematite crystals dissolve. During slow cooling, relatively large magnetoplumbite ($PbFe_{12}^{3+}O_{19}$) crystals form. Rapid cooling (quenched glazes) results in a homogeneous glaze as magnetoplumbite crystallisation is not observed. According to Roisine et al. (2017) [4], magnetoplumbite forms above 1023°C, while other studies report its formation from a mixture of Fe_2O_3 and PbO at temperatures as low as 600°C but if haematite crystallises first, magnetoplumbite crystallises only at temperatures above 800°C. The presence of magnetoplumbite has been determined in black decorations on 17th century lead-glazed colonial ceramics from Mexico [5]. Other iron-based crystals that have been identified in historic glazes are, andradite ($Ca_3Fe_2^{3+}(SiO_4)_3$) in some late 15th-early 16th century glazed tiles from Coimbra, Portugal [6] and jacobsite ($(Mn,Fe)^{2+}(Mn,Fe)_2^{3+}O_4$) in the brown decorations of 16th century Portuguese productions [7]. The precise conditions under which magnetoplumbite, andradite and jacobsite form in lead-based glazes remain unclear.

In addition, black decorations often contain manganese oxide. Kentrolite ($Pb_2Mn_2^{3+}Si_2O_9$), hausmannite (Mn_3O_4) and braunite (Mn_7SiO_{12}) crystals are found in Islamic tin-lead-glazed pottery [8,9]. Kentrolite and hausmannite are found in Hispano-Moresque pottery [10], in the oldest Swiss tin-opacified stove tiles [11] and in 16th century Portuguese productions [12]. Bustamite ($(Mn,Ca)_3Si_3O_9$) is found in medieval 10th century production in la Vega de Granada [13] and in 13–14th century Barcelona productions [9]. Braunite is found in 17th century tin-lead glazes from Portugal [14], Barcelona [9] and Hungary [15] among others.

When both manganese and iron are present, phases combining both iron and manganese are expected to form, such as Fe-kentrolite ($Pb_2(Mn,Fe)_2^{3+}Si_2O_9$) or jacobsite ($(Mn,Fe)^{2+}(Mn,Fe)_2^{3+}O_4$). In our previous research [16], we focused on studying the compounds formed by manganese oxide in glazes. The current study extends this investigation to determine the compounds formed by the combination of iron and manganese in glazes. The kinetic profile of the experiment was designed to provide insight into the sequence of iron and iron-manganese phases formed during heating and cooling.

This study aims to determine which iron and manganese compounds are formed during the firing of high lead glazes, and their possible role as fingerprints of the materials and firing conditions used in the production of black-brown decorations on lead glazes. To this end, a high-temperature powder X-ray diffraction (HT-PXRD) experiment using synchrotron radiation was designed to determine the sequence of phases formed and their stability range during heating and cooling. Mixtures of iron oxide and iron and manganese oxides with lead oxide and quartz (near eutectic high lead glass composition) are studied. To determine the role of aluminium oxide (Al_2O_3), calcium oxide (CaO), and magnesium oxide (MgO) -commonly present in historic glazes and crystalline compounds- kaolinite, calcite, and dolomite were respectively added to the mixture.

The same mixtures were fired between 850°C and 1020°C, following the same thermal path in a laboratory kiln. The resulting glazes were examined using X-ray diffraction (XRD) to identify the new crystals formed. Additionally, optical microscopy (OM) and scanning electron microscopy (SEM-EDS) were used to determine the size and shape of these crystalline phases. In this way, the iron manganese crystals in ancient lead glazes would be identified using SEM-EDS, without needing micro-XRD at the synchrotron.

2. Experimental methodology

A basic mixture of a near eutectic high lead glass, 70 wt% PbO: 30 wt % SiO_2, with the addition of 10 wt% Fe_2O_3, labelled **R7-Fe**, was prepared using minium (Pb_3O_4, Panreac 121476.1211), quartz (SiO_2, Sigma 101194530) and haematite (Fe_2O_3, Panreac 212575.1210). The exact composition is given in Table 1.

The influence of Al_2O_3 was studied by adding kaolinite ($Al_2Si_2O_5(OH)_4$, FAST ANCIL) to the above mixture, which was labelled **K7-Fe** (63.56 wt% minium, 24.67 wt% quartz and 11.76 wt% kaolinite). In addition, the influence of Ca was investigated by adding 10 wt% of calcite ($CaCO_3$, Panreac 121212.1210) mixtures labelled **K7-Fe-C.** And the influence of Mg, adding 10 wt% of dolomite ($CaMg(CO_3)_2$ (FAST ANCIL), labelled **K7-Fe-D** (see Table 1).

To further investigate the effects of the combination of manganese and iron oxides, new mixtures identical to the previous ones were prepared with the addition of 10 wt% of MnO (Panreac 211408.1210) and labelled **R7-FeMn**, **K7-FeMn**, **K7-FeMn-C** and **K7-FeMn-D**, respectively (see Table 1).

Finally, mixtures with manganese, like those containing Fe_2O_3 but with MnO instead, (**R7-Mn, K7-Mn, K7-Mn-C** and **K7-Mn-D**), previously published by Molera et al., [16], have been included for comparison.

The mixtures were ground in an agate mortar to a granulometry of less than 80 microns, which was found to be the optimum size for the subsequent High-Temperature Synchrotron Powder X-ray Diffraction (HT-XRPD) experiment. The use of coarsely ground materials will only slow down the decomposition process and shift to higher temperatures the transformations. The aim is to determine the sequence of phases that

Table 1
Calculated chemical composition of the mixtures (wt%). SiO_2 is added as quartz, PbO as minium, Al_2O_3 as kaolinite, Fe_2O_3 as haematite, MnO as manganosite, CaO as calcite and MgO as dolomite.

Reference	Mixtures	PbO	SiO_2	Al_2O_3	CaO	MgO	Fe_2O_3	MnO
R7-Fe	10 g R7 + 1 g Fe_2O_3	61.3	29.0				9.7	
K7-Fe	10 g K7 + 1 g Fe_2O_3	56.3	29.4	4.5			9.8	
K7-Fe-C	10 g K7 + 1 g Calcite + 1 g Fe_2O_3	52.9	27.6	4.3	6.0		9.2	
K7-Fe-D	10 g K7 + 1 g Dolomite + 1 g Fe_2O_3	53.5	28.0	4.3	2.8	2.0	9.3	
R7-FeMn	10 g R7 + 1 g Fe_2O_3 + 1 g MnO	55.9	26.4				8.8	8.8
K7-FeMn	10 g K7 + 1 g Fe_2O_3 + 1 g MnO	51.3	26.8	4.1			8.9	8.9
K7-FeMn-C	10 g K7 + 1 g Calcite + 1 g Fe_2O_3 + 1 g MnO	48.4	25.3	3.9	5.5		8.4	8.4
K7-FeMn-D	10 g K7 + 1 g Dolomite + 1 g Fe_2O_3 + 1 g MnO	49.0	25.6	3.9	2.6	1.9	8.5	8.5
R7-Mn	10 g R7 + 1 g MnO	61.3	29.0					9.7
K7-Mn	10 g K7 + 1 g MnO	56.3	29.4	4.5				9.8
K7-Mn-C	10 g K7 + 1 g Calcite + 1 g MnO	52.9	27.6	4.3	6.0			9.2
K7-Mn-D	10 g K7 + 1 g Dolomite + 1 g MnO	53.5	28.0	4.3	2.8	2.0		9.3

are formed under conditions that are not constrained by the kinetics of the transformation. The mixtures were introduced into a 500 μm diameter quartz capillary and HT-PXRD experiments were conducted at the high-resolution endstation of the BL04-MSPD beamline at ALBA Synchrotron. Measurements were performed in transmission mode with a rotating capillary at an energy of 30 keV (wavelength λ=0.41264 Å, determined from a Si640d NIST standard), which mitigates the strong absorption of lead-containing mixtures. Diffraction data were collected using a six-module Mythen detector, covering an angular range of 40° (2θ) with a step size of 0.006°. An FMB Oxford hot air blower was used to raise the temperature from room temperature (RT) to 400°C at a rate of 20 °C/min, to elevate it further to the maximum temperature at a rate of 10 °C/min, and then to reduce the temperature from the maximum temperature to RT at a rate of 25 °C/min. The blower temperature was calibrated using the cell parameter of silica (Si640d NIST), which was refined from diffraction data collected under identical conditions to those used for the samples. The maximum temperature reached was 928°C. During the heating and cooling stages, data acquisition was performed sequentially with an acquisition time of 10 seconds. The final temperatures (928°C and RT) were held for five minutes. In Fig. S1 the XRD patterns of heating and cooling for each sample are shown, with identification of crystalline phases.

To study the microstructure developed during firing at temperatures exceeding those reached in the HT-PXRD experiment, the mixtures were applied to a previously fired ceramic tile and fired at 850°C, 928°C, 950°C, 980°C and 1020°C. The firing was conducted using the heating ramp of 10 °C/min, with the maximum temperature maintained for 10 min. The surface was examined by both optical microscopy (OM) and scanning electron microscopy (SEM). For the SEM examination was used a cross-beam workstation (Zeiss Neon 40; Carl Zeiss AG, Oberkochen, Germany) equipped with a Schottky field emitter column with an attached Energy Dispersive Spectroscopy (EDS) detector (Ultim EDS Detector, Aztec, Oxford Instruments, Abingdon, UK) at Center for Research in Multiscale Science and Engineering (CCEM), UPC University. Backscattered electron (BSE) images were obtained and the crystallites formed were analysed using the EDS to determine their composition at 20 kV acceleration voltage with 20 nA current, 7.5 mm working distance and 120 s measurement time. The EDS was calibrated using oxide and mineral standards and a high lead glass (K229, Geller Microanalytical Laboratory, MA, USA).

The glazes fired at 950°C and 980°C were also analysed by conventional XRD (Bruker D8 Advance 3.1 Bragg-Brentano diffractometer with a PSD Lynx-Eye detector and a monochromator), using Cu Kα radiation (wavelength λ=1.5418 Å). Additionally, a thin cross-section of the samples fired at 1020°C was analysed by micro-XRD (SR-XRD) at the microdiffraction endstation of BL04-MSPD beamline at ALBA synchrotron, using 29.2 keV X-rays (λ=0.4246 Å, determined from the Sn K-edge) and a beam spot of 20 microns.

3. Results

Fig. 1 illustrates the glazes obtained for all mixtures at firing temperature of 950°C, heating ramp of 10 °C/min, and holding the maximum temperature for 10 min. The glazes comprising solely iron display a reddish-brown hue. The R7-Fe glaze exhibits a honey-brown hue, comparable to that of the K7-Fe-C and K7-Fe-D glazes, while the K7-Fe glaze displays a darker tone. Mixtures containing MnO appear dark brown, while those containing both iron and manganese appear black. R7-FeMn is mat and exhibits numerous crystalline phases on the surface. K7-FeMn is black but is slightly more vitrified, while K7-FeMn-D displays a prevalence of bubbles, potentially resulting from dolomite decomposition during firing.

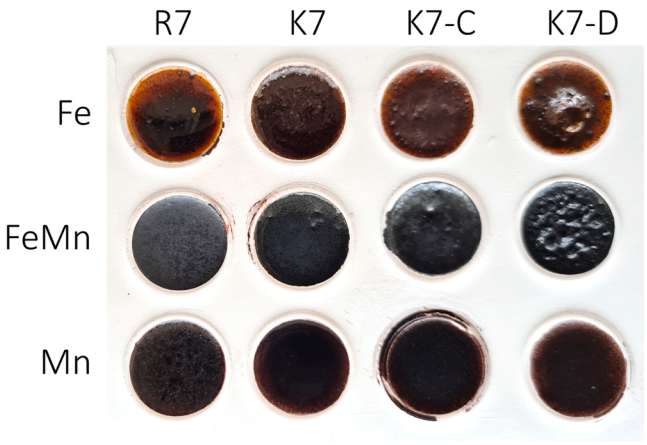

Fig. 1. Mixtures fired at 950°C at 10 °C/min keeping the maximum temperature for 10 min.

3.1. *Fe_2O_3 and MnO mixtures (R7-Fe, R7-Mn and R7-FeMn)*

3.1.1. *PbO-SiO_2-Fe_2O_3 (R7-Fe)*

The transformations occurring in PbO-SiO_2-Fe_2O_3 (R7-Fe) mixtures during the HT-PXRD experiment are shown in Fig. 2. The reaction of lead oxide with quartz results in the formation of hexagonal and monoclinic lead silicate, Pb_2SiO_4, at about 510°C, both of which melt at ≈ 695°C. At ≈ 555°C, minium (Pb_3O_4) transforms into litharge/massicot (PbO) and a lead-rich silicate, $Pb_{11}Si_3O_{17}$, is formed, which disappears at ≈ 650°C.

Upon reaction with the resulting melt, melanotekite, $Pb_2Fe^{3+}{}_2O_2(Si_2O_7)$, crystallises around the haematite particles (Fe_2O_3) at temperatures above 630°C. A silica-rich lead silicate, Fe-barysilite, $Pb_8Fe^{3+}(Si_2O_7)_3$, forms at ≈ 640°C and melts at ≈ 690°C.

Quartz does not fully react with PbO to form a melt, but some remains in its original crystalline form. In addition, a small fraction of cristobalite is formed at ≈ 760°C. The crystallisation of cristobalite at such low temperatures and once a silicate liquid is formed has been previously observed and is believed to be related to the presence of elements other than silica in the melt, such as sodium, lead [23,24] or iron [25].

The HT-PXRD synchrotron experiment for this sample was interrupted at 846°C. However, the glazes of the same composition obtained at higher temperatures have shown that melanotekite melts below 950°C, consistent with our previous studies [2]. Fig. 2 shows that after firing at 928°C abundant large crystals (visible by optical microscopy) of melanotekite with a needle-like shape are observed. At temperatures above 950°C, only hexagonal platelets of haematite and cristobalite crystals are present (along with the quartz relics), as can be seen in the SEM and confirmed by SR-XRD of the sample fired at 1020°C shown in Fig. 3.

3.1.2. *PbO-SiO_2-MnO (R7-Mn)*

The transformations occurring in the PbO-SiO_2-MnO (R7-Mn) mixture have already been published [16]. Therefore, we present only the most significant results for comparison with Fe mixtures and Fe-Mn mixtures (see Fig. 2). Minium (Pb_3O_4) reacts with quartz to produce the same sequence of lead silicate phases as found in R7-Fe (Pb_2SiO_4 and $Pb_{11}Si_3O_{17}$). At ≈ 580°C, manganosite, $Mn^{2+}O$, is converted to bixbyite, $Mn_2^{3+}O_3$. Mn-barysilite, $Pb_{2.8}Mn_{0.2}^{2+}Si_2O_7$, is formed at ≈ 650°C and melts at ≈ 750°C. Bixbyite reacts with the melt formed and at temperatures above 700°C, kentrolite, $Pb_2Mn_2^{3+}Si_2O_9$, crystallises around the manganese oxide particles. Above 950°C kentrolite decomposes, and braunite, $Mn^{2+}Mn_6^{3+}O_8SiO_4$, is formed. Cristobalite is formed at 760°C and remains up to 1020°C.

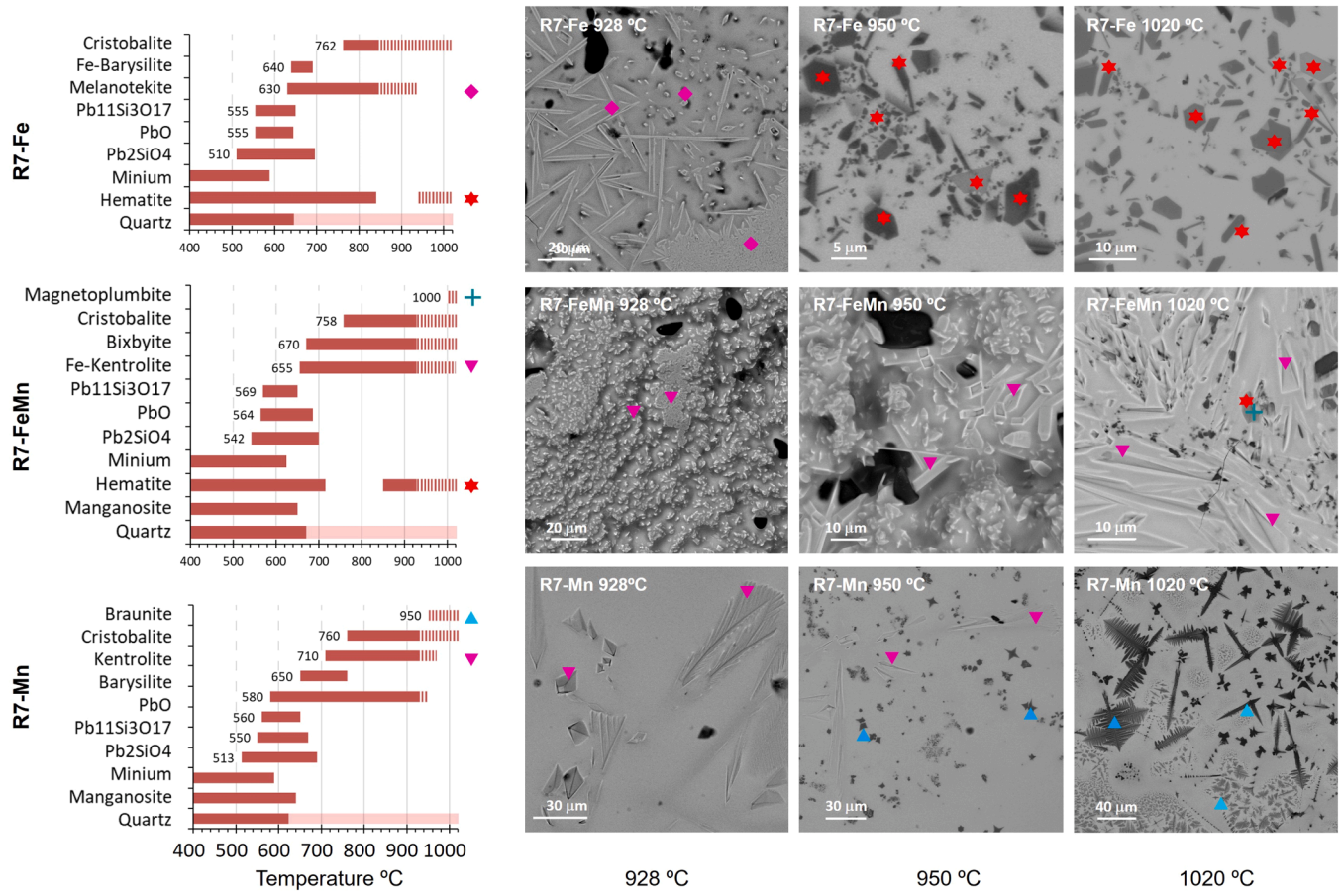

Fig. 2. (left) Sequence of crystalline phases in the R7-Fe, R7-FeMn and R7-Mn mixtures according to the synchrotron HT-PXRD experiment up to 928°C (solid bars) and crystalline phases identified by SEM and XRD (dashed bars) of samples fired at 950°C, 980°C and 1020°C. (right) SEM-BSD images of the crystalline phases at 928°C, 950°C and 1020°C.

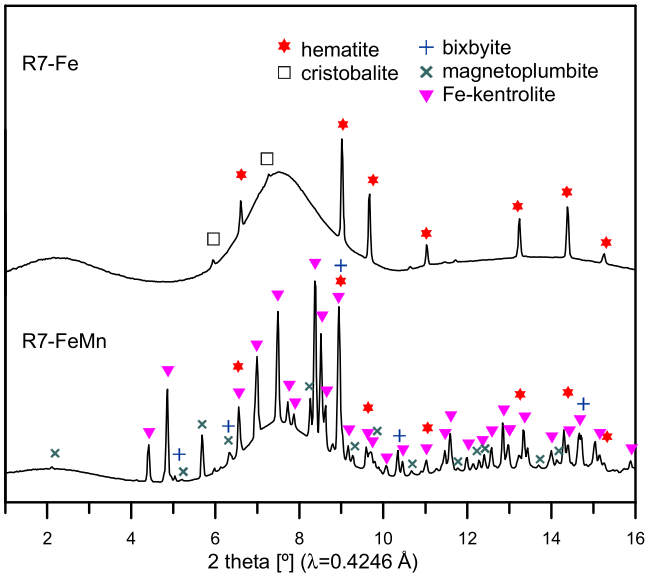

Fig. 3. SR-XRD patterns of R7-Fe and R7-FeMn fired at 1020°C.

3.1.3. *PbO-SiO_2-Fe_2O_3-MnO (R7-FeMn)*

The transformations occurring in the PbO-SiO_2-Fe_2O_3-MnO (R7-FeMn) mixture are shown in Fig. 2. The reaction of minium with quartz results in the same sequence of lead silicate phases observed in the previous mixtures, although at slightly higher temperatures. However, the most notable difference between this mixture and those previously studied is the absence of barysilite. Instead, as soon as the PbO and lead silicates disappear at ≈ 655°C, Fe-kentrolite ($Pb_2(Mn,Fe)_2^{3+}Si_2O_9$), crystallises and remains stable up to 1020°C.

Manganosite transforms to bixbyite at ≈ 670°C and is also found in the mixtures fired up to 1020°C. According to the Ellingham diagram, the oxidation of MnO would first go through Mn_3O_4 and finally bixbyite. In the diffraction patterns, it is not possible to observe the formation of Mn_3O_4, and if it does occur, it must be very rapid and masked by the complexity and the number of peaks present around 650°C. Bixbyite appears blurred in the SEM and is difficult to identify. XRD reflections corresponding to haematite disappear when Fe-kentrolite ($Pb_2(Mn,Fe)_2^{3+}Si_2O_9$) crystallises. Above 850°C, haematite recrystallises into hexagonal crystals (incorporating some Mn), although smaller in size and less abundant than in the R7-Fe mixtures. At 1020°C, the presence of magnetoplumbite, $Pb(Fe^{3+},Mn^{3+})_{12}O_{19}$, is determined by SR-XRD.

3.2. *The effect of adding kaolinite (K7-Fe, K7-Mn, K7-FeMn)*

The addition of 4.1–4.5 % of Al_2O_3 (as kaolinite) reduces the melting temperature of the near eutectic lead glaze by about 60°C, so that all the transformations take place at lower temperatures and the mixtures appear more vitrified. The results are shown in Fig. 4.

3.2.1. *PbO-SiO_2-Fe_2O_3 + kaolinite (K7-Fe)*

In the mixtures PbO-SiO_2-Al_2O_3-Fe_2O_3 (K7-Fe), minium is converted to massicot and litharge (≈ 575°C), then Pb_2SiO_4 is formed (≈ 580°C), which melts at 640°C. A lead-rich aluminosilicate, $Pb_8Al_2Si_4O_{19}$, is

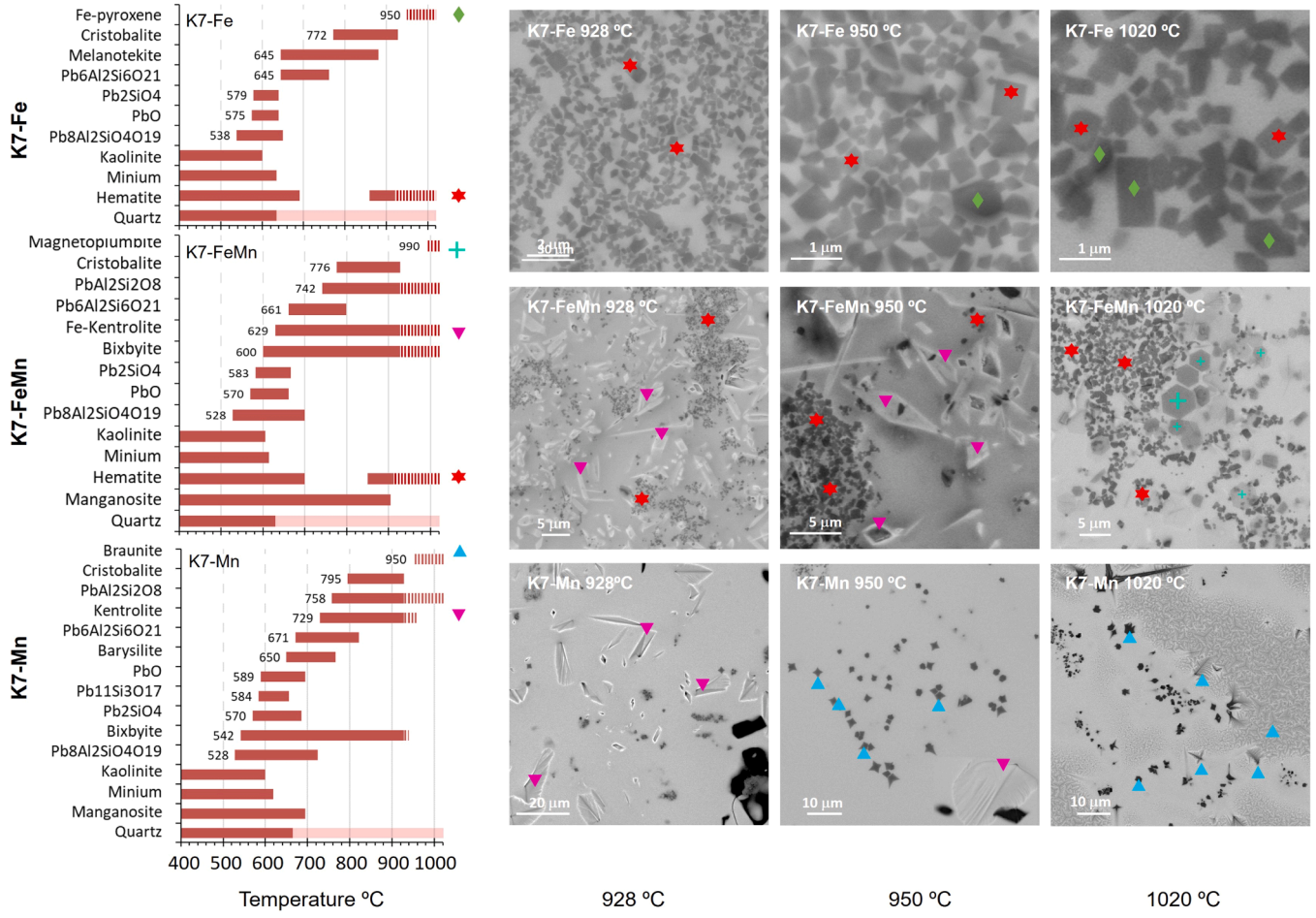

Fig. 4. (left) Crystalline phases formed in the K7-Fe, K7-FeMn and K7-Mn mixtures according to the synchrotron HT-PXRD experiment (solid bars) and identified by SEM and RT-XRD (dashed pattern). (right) SEM-BSD images of the crystalline phases at 928°C, 950°C and at 1020°C.

formed at ≈ 538°C (before Pb_2SiO_4) and disappears at ≈ 650°C. A lead-poor aluminosilicate, $Pb_6Al_2Si_6O_{21}$, and melanotekite are formed at ≈ 645°C and disappear at ≈ 760°C and ≈ 880°C respectively. Cristobalite is formed at ≈ 722°C. After cooling, only cristobalite and haematite are present in the samples fired from 928°C to 1020°C.

SEM analysis shows that the haematite crystals have a cubic shape, rather than the hexagonal platelets formed in the R7-Fe mixture. Cubic-shaped haematite is found at firing temperatures above 850°C. The size of these cubic crystals ranges from 200 to 500 nm, being larger at higher temperatures. XRD analysis shows that it has a rhombohedral α-Fe_2O_3 crystal structure (JCPDS file no. 84–0311) (Fig. 5), in good agreement with other studies that have found small cubes of rhombohedral haematite [17,18]. Given that the firing conditions are the same as for the R7-Fe mixture, the fact that the haematite crystals are now cubic instead of hexagonal should be related to the presence of kaolinite in the mixture.

3.2.2. *PbO-SiO_2-MnO + kaolinite (K7-Mn)*

The transformations occurring in the mixture PbO-SiO_2-Al_2O_3-MnO (K7-Mn) have been previously published [16], so we comment only significant results for comparing with the iron equivalents. Different lead-aluminosilicates and lead-silicates are formed ($Pb_8Al_2Si_4O_{19}$, $Pb_6Al_2Si_6O_{21}$, Pb_2SiO_4, $Pb_{11}Si_3O_{17}$), but the difference from K7-Fe mixture is the formation of lead feldspar $Pb_2AlSi_3O_8$ at temperatures as low as ≈ 760°C which persists up to 1020°C. Manganoan-barysilite, is formed at 650°C (at the same temperature as R7-Mn), kentrolite is formed at ≈ 730°C (at 710°C for R7-Mn) but in both cases persists up to 980°C. Braunite, $Mn^{2+}Mn_6^{3+}O_8SiO_4$, crystals are found at 950°C (the same temperature as R7-Mn). The main difference is in the crystal size: the braunite crystals in the kaolinitic mixture are smaller than in the equivalent mixture without kaolinite.

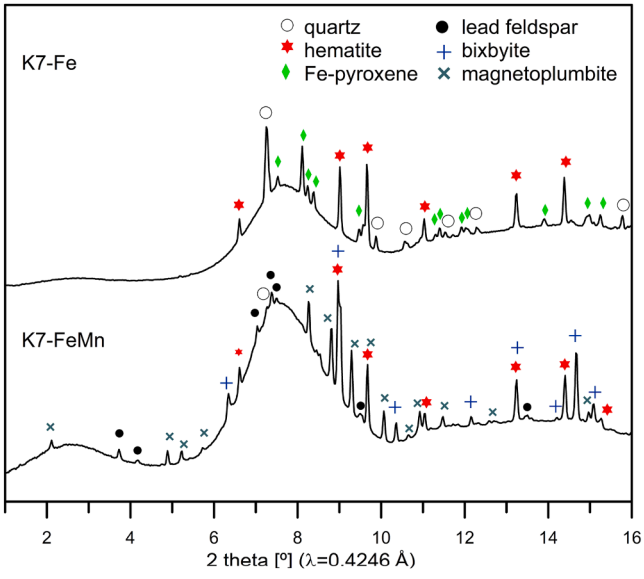

Fig. 5. SR-XRD patterns of mixture K7-Fe and K7-FeMn fired at 1020°C.

3.2.3. *PbO-SiO_2-Fe_2O_3-MnO + kaolinite (K7-FeMn)*

The transformations observed in the mixture PbO-SiO_2-Al_2O_3-Fe_2O_3-MnO (K7-FeMn) are like those of K7-Mn, with the formation of lead silicates (Pb_2SiO_4, $Pb_{11}Si_3O_{17}$) and aluminosilicates $Pb_8Al_2Si_4O_{19}$ and $Pb_6Al_2Si_6O_{21}$ and lead feldspar ($Pb_2AlSi_3O_8$). Barysilite is not formed as in the R7-FeMn mixture. Fe-kentrolite is formed at a lower temperature (≈629°C) than K7-Fe or K7-Mn and melts above 950°C. Cubic-shaped haematite are observed by SEM at 928°C and up to 1020ºC. The most remarkable difference from previous mixtures is the formation of magnetoplumbite ($Pb(Fe,Mn)^{3+}_{12}O_{19}$) crystals at 1020°C, which appear well developed and visible by OM, SEM, and also in the XRD patterns (Fig. 5).

3.3. *The effect of adding kaolinite and calcite (K7-Fe-C, K7-Mn-C, K7-FeMn-C)*

3.3.1. *PbO-SiO_2-Fe_2O_3 + kaolinite + calcite (K7-Fe-C)*

When calcite is added, mixture of PbO-SiO_2-Al_2O_3-CaO-Fe_2O_3 (K7-Fe-C), Pb_2SiO_4 and $Pb_8Al_2Si_4O_{19}$ are formed, but not $Pb_6Al_2Si_6O_{21}$ nor lead feldspar $Pb_2AlSi_3O_8$. Instead, $Pb_2Al_2SiO_6$ is formed in a similar temperature range to $Pb_6Al_2Si_6O_{21}$ in K7-Fe. Fe-barysilite, which was not formed in K7-Fe, is now formed over a wider temperature range than R7-Fe (from ≈ 635°C to ≈ 760°C). Melanotekite is formed at ≈ 660°C, a lower temperature than in R-Fe and K-Fe, and melts at ≈ 830°C (Fig. 6).

Calcite decomposes during firing, and CaO reacts forming ganomalite $Pb_9Ca_6(Si_2O_7)_3(SiO_4)_3$, a calcium lead-rich silicate in the range of ≈ 720°C to ≈ 825°C, consistent with the stable composition range proposed by Shevchenko and colleagues [19,20]. Wollastonite, $CaSiO_3$, is formed at ≈ 850°C and remains up to 1020°C.

Cubic-shaped crystals of haematite are also visible by SEM and OM between 928°C and 1020°C. In addition, the reaction between Fe_2O_3 and CaO promotes the formation of a Ca-Fe garnet, andradite $Ca_3(Fe^{3+})_2(SiO_4)_3$, at ≈ 846°C up to 1020°C, increasing in size with temperature.

3.3.2. *PbO-SiO_2-MnO + kaolinite + calcite (K7-Mn-C)*

The mixture PbO-SiO_2-Al_2O_3-CaO-MnO (K7-Mn-C) differs from the K7-Fe-C mixture in the stability range of barysilite, which increases from ≈ 600°C to ≈ 825°C. Kentrolite is also formed at slightly higher temperatures (≈ 758°C) than in K7-Mn (≈ 730°C) or R7-Mn (≈ 710°C) and melts at ≈ 950°C. (Fig. 6).

Ganomalite and wollastonite are also formed, but with the incorporation of Mn into wollastonite, it transforms into bustamite ($CaMnSi_2O_6$) at approximately 950°C, and wollastonite disappears at around 980°C. Braunite, $Mn^{2+}Mn^{3+}_6O_8SiO_4$, is formed at ≈ 950°C and remains up to 1020°C.

For the mixtures PbO-SiO_2-Al_2O_3-CaO-Fe_2O_3-MnO (K7-Fe-C), the same phases form as in K7-Fe-C: Fe-barysilite, Fe-kentrolite, ganomalite, andradite, and wollastonite. The main difference is the formation of magnetoplumbite. $Pb(Fe,Mn)^{3+}_{12}O_{19}$, at 1020°C as magnetoplumbite is only formed when both Fe and Mn are present (Fig. 6 and Fig. 7).

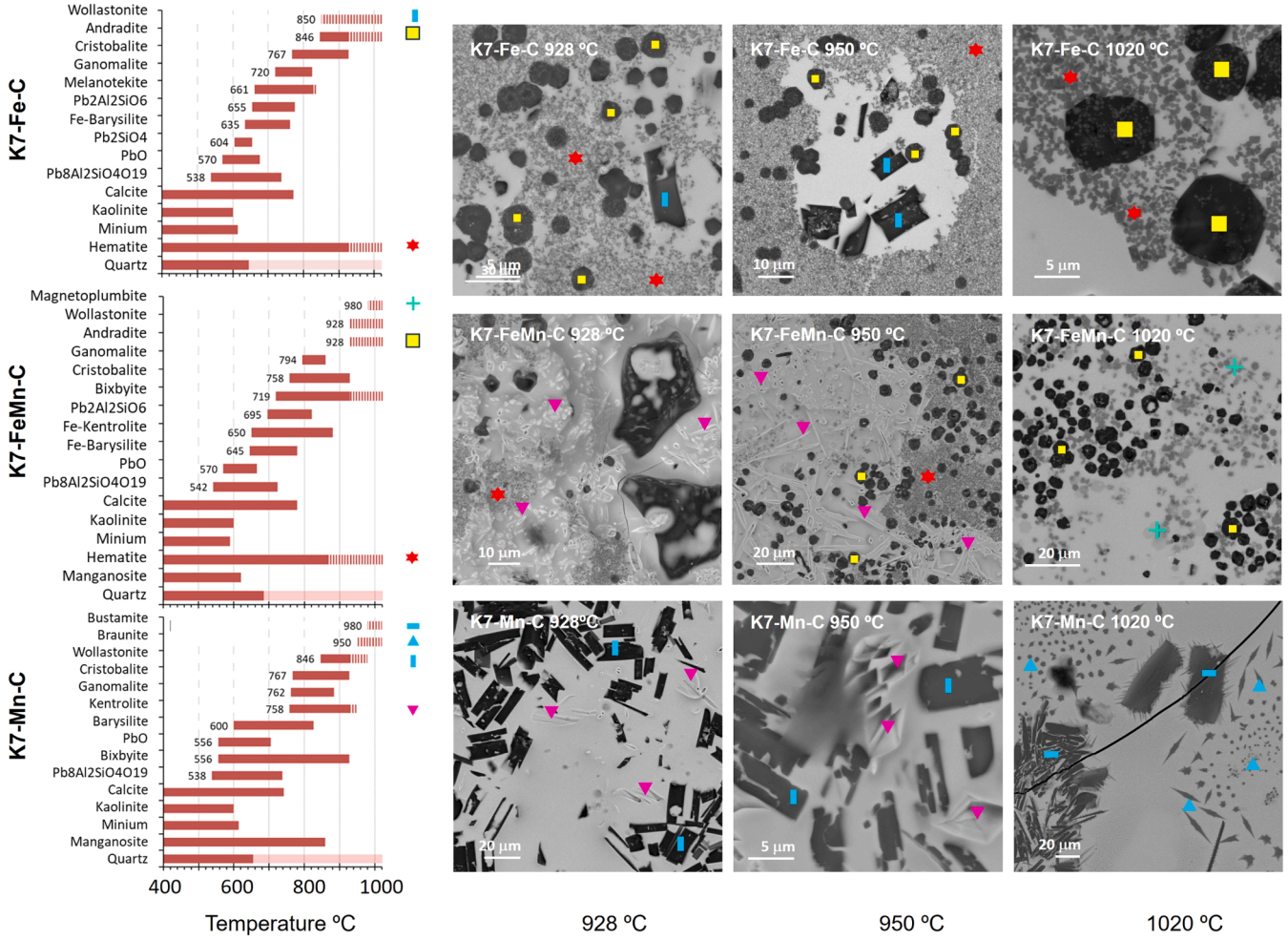

Fig. 6. (left) Crystalline phases formed in the K7-Fe-C, K7-FeMn-C and K7-Mn-C mixtures according to the synchrotron HT-XRD experiment (solid bars) and identified by SEM and RT-XRD (dashed pattern). (right) SEM-BSD images of the crystalline phases at 928°C, 950°C and at 1020°C.

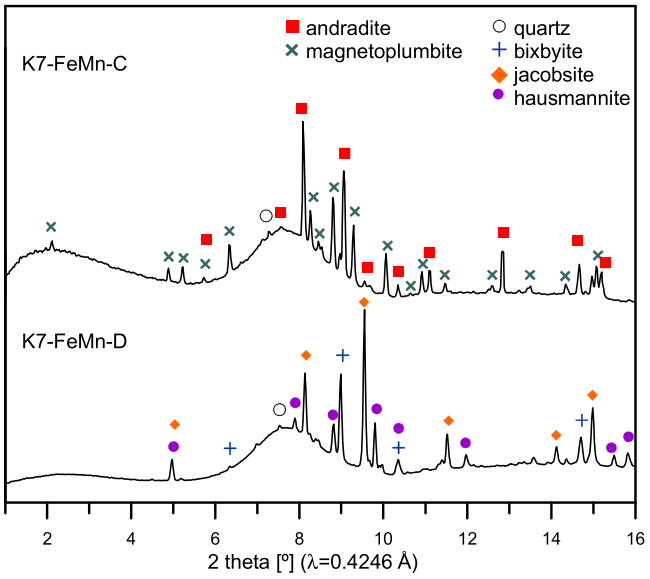

Fig. 7. SR-XRD patterns of mixture K7-FeMn-C and K7-FeMn-D fired at 1020°C.

3.4. *The effect of adding kaolinite and dolomite (K7-Fe-D, K7-Mn-D, K7-FeMn-D)*

3.4.1. *PbO-SiO_2-Fe_2O_3 + kaolinite + dolomite (K7-Fe-D)*

The addition of dolomite instead of calcite, PbO-SiO_2-Al_2O_3-CaO-MgO-Fe_2O_3 (K7-Fe-D), is intended to determine the role of Mg in the phases formed. It was not possible to measure K7-Fe-D at the ALBA synchrotron HT-XRD experiment, but it was studied by firing the mixtures at temperatures of 850°C, 928°C, 950°C, 980°C and 1020°C temperatures and analysing both the surface and cross-section of the glazes. The results obtained are shown in Fig. 8. The presence of Mg promotes the formation of pyroxene (Ca,Mg,Fe)(Si,Al)$_2O_6$ at 850°C. Only pyroxenes and cubic-shaped crystals of haematite are present at 928°C and persist up to 1020°C.

3.4.2. *PbO-SiO_2-MnO + kaolinite + dolomite (K7-Mn-D)*

The transformations occurring in the mixture PbO-SiO_2-Al_2O_3-CaO-MgO-MnO (K7-Mn-D) are the following: Mn-barysilite forms between ≈ 625°C and ≈ 789°C. Kentrolite forms at ≈ 762°C and melts at ≈ 917°C. Pyroxenes form at ≈ 800°C up to 1020°C. Braunite, $Mn^{2+}Mn_6^{3+}O_8SiO_4$, forms at ≈ 950°C growing at higher temperatures (Fig. 8).

3.4.3. *PbO-SiO_2-Fe_2O_3-MnO + kaolinite + dolomite (K7-FeMn-D)*

In the mixture PbO-SiO_2-Al_2O_3-CaO-MgO-Fe_2O_3-MnO (K7-FeMn-D) notable results are the formation of new different phases compared to previous cases. Jacobsite, $(Mn,Fe,Mg)^{2+}(Fe,Mn)_2^{3+}O_4$, is formed at ≈ 928°C and hausmannite, Mn_3O_4, above 980°C (Fig. 8). Pyroxenes (Ca,Mg,Fe,Mn)$_2$(Si,Al)$_2O_6$ and magnetoplumbite are also formed at ≈ 830°C and ≈ 950°C respectively and persist up to 1020°C. (Fig. 8).

Finally, as a summary, the stability ranges of Fe and Mn compounds, which may serve as distinctive markers for analyzing ancient ceramics, are presented in Table 2, and Fig. S2.

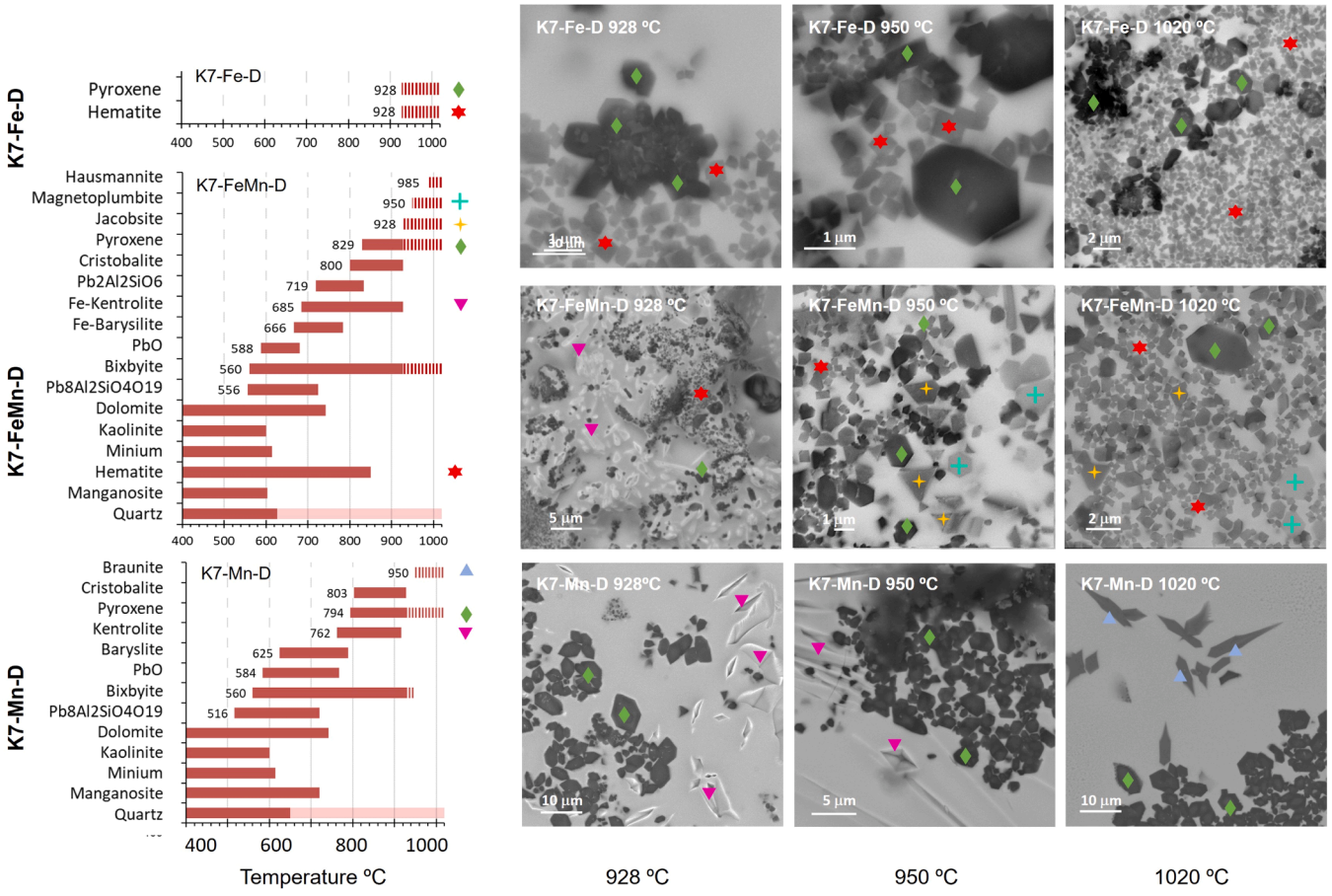

Fig. 8. (left) Crystalline phases formed in the K7-Fe-D, K7-FeMn-D and K7-Mn-D mixtures according to the synchrotron HT-XRD experiment (solid bars) and identified by SEM and RT-XRD (dashed pattern). (right) SEM-BSD images of the crystalline phases at 928°C, 950°C and at 1020°C.

Table 2
Stability ranges of Fe and Mn Compounds determined by HT-XRD. (n.d is non-detected).

Lead silicates		**R7**	**K7**	**K7-C**	**K7-D**
Pb_2SiO_4	**Fe**	510–695	579–640	604–655	
idem	**FeMn**	542–700	583–666	n.d	n.d
idem	**Mn**	513–690	570–686	n.d	n.d
$Pb_{11}Si_3O_{17}$	**Fe**	555–650	n.d	n.d	
idem	**FeMn**	569–650	n.d	n.d	n.d
idem	**Mn**	550–669	584–656	n.d	n.d
$Pb_8Al_2Si_4O_{19}$	**Fe**	-	538–650	538–738	
idem	**FeMn**	-	528–700	538–724	556–724
idem	**Mn**	-	528–724	538–738	516–720
$Pb_6Al_2Si_6O_{21}$	**Fe**	-	645–762	n.d	
idem	**FeMn**	-	661–779	n.d	n.d
idem	**Mn**	-	671–821	n.d	n.d
$Pb_2Al_2SiO_6$	**Fe**	-	n.d	655–776	
idem	**FeMn**	-	n.d	695–821	n.d
idem	**Mn**	-	n.d	n.d	n.d
$Pb_2Al_2Si_2O_8$	**Fe**	-	n.d	n.d	
idem	**FeMn**	-	742–928	n.d	n.d
idem	**Mn**	-	758–928	n.d	n.d
Silicates with Fe/Mn		**R7**	**K7**	**K7-C**	**K7-D**
Barysilite	**Fe**	640–690	n.d	635–762	
idem	**FeMn**	-	n.d	645–780	666–784
idem	**Mn**	650–760	650–767	600–826	625–789
Melanotekite	**Fe**	630–930	645–881	661–829	
Fe-Kentrolite	**FeMn**	655–1020	629–950	650–950	685–928
Kentrolite	**Mn**	710–970	729–960	758–950	762–917
Pyroxene	**Fe**	-	950–1020	n.d	850–1020
idem	**FeMn**	-	n.d	n.d	850–1020
idem	**Mn**	-	n.d	n.d	794–1020
Ganomalite	**Fe**	-	-	720–825	n.d
idem	**FeMn**	-	-	794–860	n.d
idem	**Mn**	-	-	762–885	n.d
Andradite	**Fe**	-	-	846–1020	n.d
idem	**FeMn**	-	-	850–1020	n.d
idem	**Mn**	-	-	-	-
Wollastonite	**Fe**	-	-	850–1020	n.d
idem	**FeMn**	-	-	928–1020	n.d
idem	**Mn**	-	-	846–980	n.d
Bustamite	**Fe**	-	-	-	-
idem	**FeMn**	-	-	-	nd
idem	**Mn**	-	-	980–1020	n.d
Oxides		**R7**	**K7**	**K7-C**	**K7-D**
Haematite		hexagonal platelets	cubic-shape	cubic-shape	cubic-shape
Haematite	**Fe**	920–1020	850–1020	928–1020	900–1020
idem	**FeMn**	850–1020	850–1020	850–1020	850–1020
Magnetoplumbite	**FeMn**	1000–1020	990–1020	980–1020	980–1020
Jacobsite	**FeMn**	n.d	n.d	n.d	928–1020
Bixbyite	**Mn**	580–1020	542–1020	556–1020	560–1020
Braunite	Mn	950-1020	950-1020	990-1020	950-1020

4. Discussion

The reaction of PbO and SiO_2 produces two types of lead silicates: Pb_2SiO_4 and $Pb_{11}Si_3O_{17}$. Based on the original composition of the R7 mixtures, we should be in the $PbSiO_3$-Pb_2SiO_4 phase region[21]; however, the system appears to be shifted to the left of the phase diagram (higher PbO content relative to SiO_2). This is due to the quartz not fully reacting with the melt at low temperatures. Pb_2SiO_4 ($Pb_2O{\cdot}SiO_3$ oxy-cyclosilicate) is formed ≈ 510–513°C for R7-Fe and R7-Mn respectively and ≈542°C for the R7-FeMn mixture. In all cases, this phase disappears ≈ 700°C. With the addition of kaolinite, Pb_2SiO_4 is formed at higher temperatures ≈ 575°C and disappears below 700°C (in the range 640–686°C). With the addition of calcite, this phase is only formed in a narrow range of temperatures (604–655°C) for the mixture with iron oxide (K7-Fe-C).

$Pb_{11}Si_3O_{17}$ ($(Pb_{11}O_6(Si_2O_7)(SiO_4)$), is formed at a slightly higher temperature than Pb_2SiO_4 for R7 mixtures, ≈ 550°C, but disappears at a lower temperature than Pb_2SiO_4, ≈ 650°C. With the addition of kaolinite, this phase is only formed in the K7-Mn mixture between ≈ 580°C and ≈ 656°C.

With the addition of kaolinite, system PbO-SiO_2-Al_2O_3, four lead aluminosilicates are formed: $Pb_8Al_2Si_4O_{19}$, $Pb_6Al_2Si_6O_{21}$, $Pb_2Al_2SiO_6$ and $Pb_2AlSi_3O_8$. $Pb_8Al_2Si_4O_{19}$ is the first phase formed in all mixtures in slightly different ranges: between ≈ 538°C and ≈ 738°C for K7 mixtures containing Fe, ≈ 516°C and ≈ 738°C for mixtures containing Mn and ≈ 528ºC and ≈ 724ºC for FeMn mixtures. The presence of calcite increases the temperature of formation and melting of this phase.

$Pb_6Al_2Si_6O_{21}$ is only formed in kaolinitic mixtures without calcite or dolomite: K7-Fe (≈ 645°C–762°C), K7-Mn (≈ 671°C – 821°C) and K7-FeMn (≈ 661°C–799°C) mixtures. Lead feldspar $Pb_2AlSi_3O_8$ is only formed in manganese mixtures: K7-Mn (≈ 758ºC–928°C) and K7-FeMn (≈ 742°C–928°C).

With the addition of calcite or dolomite, the last two phases ($Pb_6Al_2Si_6O_{21}$, $Pb_2AlSi_3O_8$) are not formed. On the contrary, the presence of calcite and dolomite promotes the formation of a new phase: $Pb_2Al_2SiO_6$, formed in the range ≈ 655°C–776°C for K7-Fe-C and

≈ 695–821ºC for K7-FeMn-C, and ≈ 719°C–834°C for K7-FeMn-D.

Concerning the Fe oxide, haematite (Fe_2O_3) remains largely unchanged until it reacts with the melt, leading to the formation of iron lead silicates, such as Fe-barysilite ($Pb_8Fe^{3+}(Si_2O_7)_3$) and melanotekite ($Pb_2Fe_2^{3+}O_2(Si_2O_7)$). When these phases melt, new crystals of haematite form as hexagonal platelets in the R7-Fe mixtures, whereas cubic-shaped haematite crystals are observed in all other mixtures containing Al_2O_3. Based on their cubic morphology, these crystals could be confused with magnetite or maghemite. However, XRD analysis clearly shows that they have a rhombohedral structure. Nanocubic-shaped haematite crystals have been described by other authors [17,21]. The growth of α-Fe_2O_3 cubes has been attributed to a combination of two main crystallisation mechanisms: oriented aggregation and Ostwald ripening [17]. In all K7 mixtures, cubic-shaped haematites are formed, and can be attributed to the presence of Al^{3+}. Li et al.[22], while investigating the role of Al substitution in haematite morphology, attributed this change to the smaller ionic radius and weaker electronegativity of Al^{3+} compared to Fe^{3+}.

Melanotekite ($Pb_2Fe_2^{3+}O_2(Si_2O_7)$) is the first iron lead silicate formed during firing, from ≈ 630°C for R7-Fe to ≈ 660ºC for K7-Fe-C, which is lower than the temperature 650–700°C found by Glasser [23]. It is formed in iron mixtures R7-Fe, K7-Fe and K7-Fe-C as needle-shaped crystals and decomposes at temperatures above 928°C for R7-Fe and lower temperatures for kaolinitic mixtures (≈ 881°C for K7-Fe and ≈ 829°°C for K7-Fe-C). In a previous study [2], we found that melanotekite and haematite coexist at 928°C, and only haematite is present at ≈ 950°C for mixtures of PbO-SiO_2-Fe_2O_3. This result agrees with the SEM analysis of the R7-Fe mixture.

With the addition of manganese oxide Fe-Kentrolite is formed instead melanotekite. Kentrolite and melanotekite form a solid solution [24]. In mixtures with only Mn (R7-Mn) kentrolite is formed at ≈ 7100°C melts above 900°C and, if fired below 980°C, recrystallises on cooling with a different crystal habit (feather-like instead of prismatic) [16]. In mixtures with both Fe and Mn (R7-FeMn) Fe-kentrolite is formed at ≈ 655°C and persists at 1020°C, while in kaolinitic mixture (K7-FeMn) Fe-kentrolite forms at 629ºC and melts at ≈ 950°C and does not recrystallize during cooling.

Mn-barysilite ($Pb_8Mn^{3+}(Si_2O_7)_3$) is formed in all the manganese mixtures and Fe-barysilite ($Pb_8Fe^{3+}(Si_2O_7)_3$) is formed between ≈ 640°C–690°C in R7-Fe, K7-Fe-C, K7-FeMn-C and ($Pb_8(Fe^{3+}$, Mn^{3+})$(Si_2O_7)_3$) for K7-FeMn-D. But barysilite is not formed in the mixtures K7-Fe, K7-FeMn or R7-FeMn. For these mixtures melanotekite and Fe-kentrolite are formed at low temperatures (≈ 650°C), whereas for manganese mixtures, kentrolite is formed above 710°C. Fe promotes the formation of melanotekite and Fe-kentrolite at lower temperatures than kentrolite in the Mn mixtures. Calcium is known to stabilise barysilite [25] and is formed in all the mixtures with calcite.

Hexagonal platelet crystals of magnetoplumbite ($PbFe_{12}^{3+}O_{19}$) are well developed above 980°C in mixtures containing both Fe and Mn (R7-FeMn, K7-FeMn, K7-FeMn-C, K7-FeMn-D). This is consistent with the findings reported by Roisine et al.[4], which observed the formation of relatively large magnetoplumbite crystals during slow cooling in samples fired at 1023°C.

The addition of calcite promotes the formation of ganomalite, $Pb_9Ca_6(Si_2O_7)_4(SiO_4)O$, in kaolinitic mixture (K7-Fe-C, K7-Mn-C and K7-FeMn-C) between ≈ 720°C and ≈ 764°C. For iron mixtures (K7Fe-C and K7-FeMn-C) ganomalite melts at ≈ 825°C and ≈ 860°C respectively. Above 850°C, andradite ($Ca_3Fe_2^{3+}(SiO_4)_3$) is formed and it is stable up to 1020°C. Wollastonite is formed in all Ca-containing mixtures at 850ºC for K7-Fe-C and K7-Mn-C and at higher temperatures for K7-FeMn-C (≈928°C). In the manganese mixtures, wollastonite incorporates manganese and transforms into bustamite over 990°C [16].

With the addition of dolomite, pyroxenes $(Ca,Mg,Fe,Mn)_2(Si,Al)_2O_6$ are formed above 800°C in all the mixtures. Mg promotes the crystallisation of diopside-type pyroxenes in the presence of Fe and Mn, and no other silicates are formed. In the K7-FeMn-D mixture, jacobsite ($(Mn,Fe)^{2+}(Mn,Fe)_2^{3+}O_4$) forms at ≈ 928°C and magnetoplumbite ($PbFe_{12}^{3+}O_{19}$) at ≈ 980°C.

5. Conclusions

The study of the formation and stability of different crystalline phases in mixtures of Fe, Mn, and Fe-Mn oxides and near eutectic PbO-SiO_2 with kaolinite, calcite and dolomite has provided information on the reactions and the sequence of crystalline compounds formed.

The haematite, Fe_2O_3, already present in the mixtures recrystallises as hexagonal platelets in the PbO-SiO_2 mixtures and as cubic-shaped crystals in the kaolinitic (PbO-SiO_2-Al_2O_3) mixtures. In both cases, it is stable up to 1020°C.

Barysilite, $Pb_8(Fe,Mn)^{3+}(Si_2O_7)_3$, which seems to be more stable in the calcitic mixtures with Mn forms above 600°C and disappears below 826°C.

Elongated crystals of melanotekite, $Pb_2Fe_2^{3+}O_2(Si_2O_7)$, form in the mixtures with Fe around 650°C and disappear below 930°C, or at slightly lower temperatures for kaolinitic mixtures. Prismatic crystals of kentrolite, $Pb_2Mn_2^{3+}Si_2O_9$, form in the mixtures with Mn while, Fe-kentrolite, $Pb_2(Mn,Fe)_2^{3+}Si_2O_9$, form in the mixtures with Fe and Mn and, all of them melt above 950°C. Kentrolite recrystallises on cooling only in the PbO-SiO_2 glazes fired at 980°C with a different crystal habit (feathery instead of prismatic).

In parallel, pyroxene, $(Ca,Mg,Fe,Mn)_2(Si,Al)_2O_6$, forms above 800°C in all dolomitic mixtures, and andradite, $Ca_3Fe_3^{+2}(SiO_4)_3$, forms only in calcitic mixtures with Fe above 850°C. Both are stable up to 1020°C.

When kentrolite decomposes, braunite, $Mn^{2+}Mn_6^{3+}O_8SiO_4$, forms (>950°C) in mixtures with Mn. Hexagonal platelet crystals of magnetoplumbite, $PbFe_{12}^{3+}O_{19}$, form (> 980°C) only in mixtures with both Fe and Mn. Jacobsite, $(Mn,Fe)^{2+}(Mn,Fe)_2^{3+}O_4$, forms (> 928°C) only in dolomitic mixtures with Fe and Mn. All three are stable up to 1020°C.

CRediT authorship contribution statement

J. Molera:Writing – original draft, Validation, Supervision, Methodology, Investigation, Funding acquisition, Formal analysis, Data curation, Conceptualization. **M. Colomer**:Validation, Software, Data curation. **O. Vallcorba**:Visualization, Validation, Software, Methodology, Data curation. **T. Pradell**:Writing – original draft, Validation, Supervision, Investigation, Funding acquisition, Formal analysis, Data curation, Conceptualization.

Declaration of Generative AI and AI-assisted technologies in the writing process

During the preparation of this work, the author(s) used ChatGPT only to revise the English writing. After using this tool/service, the author(s) reviewed and edited the content as needed and take(s) full responsibility for the content of the publication.

Declaration of Competing Interest

The authors declare that they have no known competing financial interests or personal relationships that could have appeared to influence the work reported in this paper.

Acknowledgements

J.M. and T.P. are grateful to the project PID2022–137783OB-I00 funded by the Ministerio de Ciencia e Innovación (Spain) and T.P. is grateful to Generalitat de Catalunya grant 2021SGR-00343. The experiments were performed at BL04 MSPD Beamline at ALBA Synchrotron Facility with the collaboration of Alba Staff, project number 2020094579.

Appendix A. Supporting information

Supplementary data associated with this article can be found in the online version at doi:10.1016/j.jeurceramsoc.2025.117244.

References

[1] T. Pradell, J. Molera, Ceramic technology. How to characterise ceramic glazes, Archaeol. Anthr. Sci. 12 (2020) 189, https://doi.org/10.1007/s12520-020-01136-9.

[2] R. Di Febo, J. Molera, T. Pradell, O. Vallcorba, C. Capelli, Technological implications of neo-formed haematite crystals in ceramic lead glazes, Sci. Technol. Archaeol. Res 3 (2017) 366–375, https://doi.org/10.1080/20548923.2017.1419675.

[3] H. Duan, M. Guan, Y. Yang, J. Jiang, W. Qian, Non-destructive identification of iron oxide crystals in 15th century A.D. Chinese imperial red overglaze decoration, J. Archaeol. Sci. Rep. 58 (2024) 104733, https://doi.org/10.1016/j.jasrep.2024.104733.

[4] G. Roisine, N. Capobianco, D. Caurant, G. Wallez, A. Bouquillon, O. Majérus, L. Cormier, S. Gilette, A. Gerbier, The art of Bernard Palissy (1510–1590): influence of firing conditions on the microstructure of iron-colouGred high-lead glazes, Appl. Phys. A Mater. Sci. Process 123 (2017) 501, https://doi.org/10.1007/s00339-017-1089-9.

[5] J.G. Iñañez, M. Madrid-Fernández, J. Molera, R.J. Speakman, T. Pradell, Potters and pigments: preliminary technological assessment of pigment recipes of American majolica by synchrotron radiation micro-X-ray diffraction (Sr-μXRD), J. Archaeol. Sci. 40 (2013) 1408–1415, https://doi.org/10.1016/j.jas.2012.09.015.

[6] S. Coentro, R.A.A. Trindade, J. Mirão, A. Candeias, L.C. Alves, R.M.C. Silva, V.S. F. Muralha, Hispano-Moresque ceramic tiles from the Monastery of Santa Clara-a-Velha (Coimbra, Portugal), J. Archaeol. Sci. 41 (2014) 21–28, https://doi.org/10.1016/j.jas.2013.07.031.

[7] S. Coentro, R.C. Da Silva, C. Relvas, T. Ferreira, J. Mirão, A. Pleguezuelo, R. Trindade, V.S.F. Muralha, Mineralogical characterization of Hispano-Moresque Glazes: a μ-Raman and scanning electron microscopy with X-Ray energy dispersive spectrometry (SEM-EDS) study, Microsc. Microanal. 24 (2018) 300–309, https://doi.org/10.1017/S1431927618000338.

[8] T. Pradell, G. Molina, J. Molera, J. Pla, A. Labrador, The use of micro-XRD for the study of glaze color decorations, Appl. Phys. A Mater. Sci. Process 111 (2013) 121–127, https://doi.org/10.1007/s00339-012-7445-x.

[9] J. Molera, J. Coll, A. Labrador, T. Pradell, Manganese brown decorations in 10th to 18th century Spanish tin glazed ceramics, Appl. Clay Sci. 82 (2013) 86–90, https://doi.org/10.1016/j.clay.2013.05.018.

[10] S. Coentro, L.C. Alves, C. Relvas, T. Ferreira, J. Mirão, J. Molera, T. Pradell, R.A. A. Trindade, R.C. Da Silva, V.S.F. Muralha, The glaze technology of Hispano-Moresque ceramic tiles: a comparison between Portuguese and Spanish collections, Archaeometry 59 (2017) 667–684, https://doi.org/10.1111/arcm.12280.

[11] M. Maggetti, SEM study of black, blue, violet and yellow inglaze colours of the oldest Swiss tin-opacified stove tiles (*c.*1450– *c.*1512, canton Bern)*, Archaeometry 63 (2021) 721–737, https://doi.org/10.1111/arcm.12638.

[12] L.F. Vieira Ferreira, D.P. Ferreira, D.S. Conceição, L.F. Santos, M.F.C. Pereira, T. M. Casimiro, I. Ferreira Machado, Portuguese tin-glazed earthenware from the 17th century. Part 2: a spectroscopic characterization of pigments, glazes and pastes of the three main production centers, Spectrochim. Acta A Mol. Biomol. Spectrosc. 149 (2015) 285–294, https://doi.org/10.1016/j.saa.2015.04.090.

[13] J. Molera, J.C. Carvajal López, G. Molina, T. Pradell, Glazes, colourants and decorations in early Islamic glazed ceramics from the Vega of Granada (9th to 12th centuries CE), J. Archaeol. Sci. Rep. 21 (2018) 1141–1151, https://doi.org/10.1016/j.jasrep.2017.05.017.

[14] S. Coentro, J.M. Mimoso, A.M. Lima, A.S. Silva, A.N. Pais, V.S.F. Muralha, Multi-analytical identification of pigments and pigment mixtures used in 17th century Portuguese azulejos, J. Eur. Ceram. Soc. 32 (2012) 37–48, https://doi.org/10.1016/j.jeurceramsoc.2011.07.021.

[15] B. Bajnóczi, G. Nagy, M. Tóth, I. Ringer, A. Ridovics, Archaeometric characterization of 17th-century tin-glazed Anabaptist (Hutterite) faience artefacts from North-East-Hungary, J. Archaeol. Sci. 45 (2014) 1–14, https://doi.org/10.1016/j.jas.2014.01.030.

[16] J. Molera, M. Colomer, O. Vallcorba, T. Pradell, Manganese crystalline phases developed in high lead glazes during firing, J. Eur. Ceram. Soc. 42 (2022) 4006–4015, https://doi.org/10.1016/j.jeurceramsoc.2022.03.028.

[17] B. Jia, L. Gao, Growth of well-defined cubic haematite single crystals: oriented aggregation and Ostwald ripening, Cryst. Growth Des. 8 (2008) 1372–1376, https://doi.org/10.1021/cg070300t.

[18] A. Umar, A.A. Ibrahim, R. Kumar, H. Albargi, M.A. Alsaiari, F. Ahmed, Cubic shaped haematite (α-Fe_2O_3) micro-structures composed of stacked nanosheets for rapid ethanol sensor application, Sens. Actuators B Chem. 326 (2021) 128851, https://doi.org/10.1016/j.snb.2020.128851.

[19] M. Shevchenko, E. Jak, Thermodynamic optimization of the binary PbO–CaO and ternary PbO-CaO–SiO_2 systems, CALPHAD 70 (2020), https://doi.org/10.1016/j.calphad.2020.101807.

[20] M. Shevchenko, L. Chen, E. Jak, experimental phase equilibria study and thermodynamic modelling of the PbO-"FeO"-SiO_2, PbO-"FeO"-CaO and PbO-"FeO"-CaO-SiO_2 systems in equilibrium with metallic Pb and Fe, J. Phase Equilibria Diffus. (2021) 452–467.

[21] M. Shevchenko, E. Jak, Experimental phase equilibria studies of the PbO–SiO_2 system, J. Am. Ceram. Soc. 101 (2018) 458–471, https://doi.org/10.1111/jace.15208.

[22] W. Li, X. Liang, P. An, X. Feng, W. Tan, G. Qiu, H. Yin, F. Liu, Mechanisms on the morphology variation of haematite crystals by Al substitution: the modification of Fe and O reticular densities, Sci. Rep. 6 (2016) 35960, https://doi.org/10.1038/srep35960.

[23] F.P. Glasser, New data on Kentrolite and Melanotekite: ternary phase relations in the system PbO-Fe_2O_3-SiO_2, Am. Mineral. 52 (1967) 1085–1093.

[24] G. Dorsam, A. Liebscher, B. Wunder, G. Franz, Crystal structures of synthetic melanotekite ($Pb_2Fe_2Si_2O_9$), kentrolite ($Pb_2Mn_2Si_2O_9$), and the aluminium analogue ($Pb_2Al_2Si_2O_9$), Am. Mineral. 93 (2008) 573–583, https://doi.org/10.2138/am.2008.2594.

[25] M. Shevchenko, E. Jak, Thermodynamic optimization of the binary PbO–CaO and ternary PbO–CaO–SiO_2 systems, CALPHAD 70 (2020), https://doi.org/10.1016/j.calphad.2020.101807.